FERMILAB-PUB-11-834-E

Test of Lorentz and CPT violation with Short Baseline Neutrino Oscillation Excesses

A. A. Aguilar-Arevalo[14], C. E. Anderson[19], A. O. Bazarko[16], S. J. Brice[8], B. C. Brown[8], L. Bugel[13], J. Cao[15], L. Coney[6], J. M. Conrad[13], D. C. Cox[10], A. Curioni[19], R. Dharmapalan[1], Z. Djurcic[2], D. A. Finley[8], B. T. Fleming[19], R. Ford[8], F. G. Garcia[8], G. T. Garvey[11], J. Grange[9], C. Green[8,11], J. A. Green[10,11], T. L. Hart[5], E. Hawker[4,11], W. Huelsnitz[11], R. Imlay[12], R. A. Johnson[4], G. Karagiorgi[13], P. Kasper[8], T. Katori[10,13], T. Kobilarcik[8], I. Kourbanis[8], S. Koutsoliotas[3], E. M. Laird[16], S. K. Linden[19],J. M. Link[18], Y. Liu[15], Y. Liu[1], W. C. Louis[11], K. B. M. Mahn[6], W. Marsh[8], C. Mauger[11], V. T. McGary[13], G. McGregor[11], W. Metcalf[12], P. D. Meyers[16], F. Mills[8], G. B. Mills[11], J. Monroe[6], C. D. Moore[8], J. Mousseau[9], R. H. Nelson[5], P. Nienaber[17], J. A. Nowak[12], B. Osmanov[9], S. Ouedraogo[12], R. B. Patterson[16], Z. Pavlovic[11], D. Perevalov[1,8], C. C. Polly[8], E. Prebys[8], J. L. Raaf[4], H. Ray[9], B. P. Roe[15], A. D. Russell[8], V. Sandberg[11], R. Schirato[11], D. Schmitz[8], M. H. Shaevitz[6], F. C. Shoemaker[16*], D. Smith[7], M. Soderberg[19], M. Sorel[6†], P. Spentzouris[8], J. Spitz[19], I. Stancu[1], R. J. Stefanski[8], M. Sung[12], H. A. Tanaka[16], R. Tayloe[10], M. Tzanov[12], R. G. Van de Water[11], M. O. Wascko[12‡], D. H. White[11], M. J. Wilking[5], H. J. Yang[15], G. P. Zeller[8], E. D. Zimmerman[5]

(The MiniBooNE Collaboration)

[1] *University of Alabama; Tuscaloosa, AL 35487*
[2] *Argonne National Laboratory; Argonne, IL 60439*
[3] *Bucknell University; Lewisburg, PA 17837*
[4] *University of Cincinnati; Cincinnati, OH 45221*
[5] *University of Colorado; Boulder, CO 80309*
[6] *Columbia University; New York, NY 10027*
[7] *Embry Riddle Aeronautical University; Prescott, AZ 86301*
[8] *Fermi National Accelerator Laboratory; Batavia, IL 60510*
[9] *University of Florida; Gainesville, FL 32611*
[10] *Indiana University; Bloomington, IN 47405*
[11] *Los Alamos National Laboratory; Los Alamos, NM 87545*
[12] *Louisiana State University; Baton Rouge, LA 70803*
[13] *Massachusetts Institute of Technology; Cambridge, MA 02139*
[14] *Instituto de Ciencias Nucleares, Universidad Nacional Autónoma de México, D.F. 04510, México*
[15] *University of Michigan; Ann Arbor, MI 48109*
[16] *Princeton University; Princeton, NJ 08544*
[17] *Saint Mary's University of Minnesota; Winona, MN 55987*
[18] *Virginia Polytechnic Institute & State University; Blacksburg, VA 24061*
[19] *Yale University; New Haven, CT 06520*

(Dated: September 19, 2011)

The sidereal time dependence of MiniBooNE ν_e and $\bar{\nu}_e$ appearance data are analyzed to search for evidence of Lorentz and CPT violation. An unbinned Kolmogorov-Smirnov test shows both the ν_e and $\bar{\nu}_e$ appearance data are compatible with the null sidereal variation hypothesis to more than 5%. Using an unbinned likelihood fit with a Lorentz-violating oscillation model derived from the Standard Model Extension (SME) to describe any excess events over background, we find that the ν_e appearance data prefer a sidereal time-independent solution, and the $\bar{\nu}_e$ appearance data slightly prefer a sidereal time-dependent solution. Limits of order 10^{-20} GeV are placed on combinations of SME coefficients. These are the best limits of SME coefficients for $\nu_\mu \to \nu_e$ and $\bar{\nu}_\mu \to \bar{\nu}_e$ oscillations. The fit values and limits of combinations of SME coefficients are provided.

PACS numbers: 11.30.Cp, 14.60Pq, 14.60.St

Violation of Lorentz invariance and CPT symmetry is a predicted phenomenon of Planck scale physics, especially with a spontaneous violation [1], and it does not require any modifications in quantum field theory or general relativity. Since neutrino oscillation experiments are natural interferometers, they can serve as sensitive probes of space-time structure. Neutrino oscillations have the potential to provide the first experimental evidence for Lorentz and CPT violation through evidence of oscilla-

*deceased
†Present address: IFIC, Universidad de Valencia and CSIC, Valencia 46071, Spain
‡Present address: Imperial College; London SW7 2AZ, United Kingdom

Operated by Fermi Research Alliance, LLC under Contract No. De-AC02-07CH11359 with the United States Department of Energy.

tions that deviate from the standard L/E dependence [2], or that show sidereal time dependent oscillations as a consequence of a preferred direction in the universe [3].

In this paper, we test the MiniBooNE $\nu_\mu \to \nu_e$ and $\bar{\nu}_\mu \to \bar{\nu}_e$ oscillation data [4, 5] for the presence of a Lorentz violation signal. Similar analyses have been performed in other oscillation experiments, including LSND [6], MINOS [7], and IceCube [8]. Naively, experiments with longer baselines and higher energy neutrinos would be expected to have better sensitivity to Lorentz violation, because small Lorentz violating terms are more prominent at high energy, where neutrino mass terms are negligible. However, some Lorentz violating neutrino oscillation models mimic the standard massive neutrino oscillation energy dependence [9]. In this case, one can expect sidereal variations in short baseline, low energy neutrino oscillation experiments.

MiniBooNE is a ν_e ($\bar{\nu}_e$) appearance short baseline neutrino oscillation experiment at Fermilab. Neutrinos are created by the Booster Neutrino Beamline (BNB), which produces a 93% (83%) pure ν_μ ($\bar{\nu}_\mu$) beam in neutrino (anti-neutrino) mode, determined by the polarity of the magnetic focusing horn. The MiniBooNE Cherenkov detector, a 12.2 m diameter sphere filled with mineral oil, is used to detect charged particles from neutrino interactions and is located 541 m from the neutrino production target. It is equipped with 1,280 8" PMTs in an optically separated inner volume, and 240 8" veto PMTs in an outer veto region. Details of the detector and the BNB can be found elsewhere [10, 11]. Charged leptons created by neutrino interactions in the detector produce Cherenkov photons, which are used to reconstruct charged particle tracks [12]. The measured angle and kinetic energy of charged leptons from neutrino interactions are used to reconstruct the neutrino energy, E_ν^{QE}, for each event, under the assumption that the target nucleon is at rest inside the nucleus and the interaction type is a charged current quasielastic (CCQE) interaction [13].

For this analysis, we use the background and error estimates from [14]. For neutrino mode, data from 6.46×10^{20} protons on target (POT) are used. An excess in the "low energy" region ($200< E_\nu^{QE}(\mathrm{MeV})<475$) was observed, with 544 events reported as compared to the prediction, $409.8 \pm 23.3(\mathrm{stat.})\pm38.3(\mathrm{syst.})$. Interestingly, this excess does not show the expected L/E energy dependence of a simple two massive neutrino oscillation model. Additionally, it is not consistent with the energy region expected for the "LSND" signal [15]. For the anti-neutrino mode analysis (5.66×10^{20}POT), MiniBooNE observed a small excess in the low energy region, and an excess in the region $475< E_\nu^{QE}(\mathrm{MeV})<1300$. The excess in this "high energy" region is found to be consistent with the LSND signal, assuming a two massive neutrino hypothesis, but remains statistically marginal. In the "combined" region ($200< E_\nu^{QE}(\mathrm{MeV})<1300$), MiniBooNE observed 241 $\bar{\nu}_e$ candidate events as compared to the prediction, $200.7 \pm 15.5(\mathrm{stat.})\pm14.3(\mathrm{syst.})$.

Although the conflict between MiniBooNE neutrino and anti-neutrino mode results can be resolved in models without CPT violation [16], CPT violation is a viable option. Since CPT violation necessarily implies violation of Lorentz invariance within interactive quantum field theory [17], we are in a well-motivated position to search for Lorentz and CPT violation using the MiniBooNE data. In fact, proposed models motivated by Lorentz violation [18, 19] can already accommodate world data including the MiniBooNE and LSND excesses with a small number of free parameters. Evidence for sidereal variation in the MiniBooNE excesses would provide a distinctive direct signal of Lorentz violation.

We use the Standard Model Extension (SME) formalism for the general search for Lorentz violation [20]. The SME is an effective quantum field theory, and the minimum extension of the Standard Model including particle Lorentz and CPT violation [20]. A variety of data have been analyzed under this formalism [21], including neutrino oscillations [6–8]. In the SME formalism, the evolution of a neutrino can be described by an effective Hamiltonian [3],

$$(h^\nu_{\mathrm{eff}})_{ab} \sim \frac{1}{E}[(a_L)^\mu p_\mu - (c_L)^{\mu\nu} p_\mu p_\nu]_{ab} \ . \qquad (1)$$

Here, E and p_μ are the energy and the 4-momentum of a neutrino, and $(a_L)^\mu_{ab}$ and $(c_L)^{\mu\nu}_{ab}$ are CPT-odd and CPT-even SME coefficients in the flavor basis. Under the assumption that the baseline is short compared to the oscillation length [22], the $\nu_\mu \to \nu_e$ oscillation probability takes the form,

$$P \simeq \frac{L^2}{(\hbar c)^2}|(\mathcal{C})_{e\mu} + (\mathcal{A}_s)_{e\mu}\sin\omega_\oplus T_\oplus + (\mathcal{A}_c)_{e\mu}\cos\omega_\oplus T_\oplus + (\mathcal{B}_s)_{e\mu}\sin 2\omega_\oplus T_\oplus + (\mathcal{B}_c)_{e\mu}\cos 2\omega_\oplus T_\oplus|^2. \qquad (2)$$

This probability is a function of sidereal time $T_\oplus$. Four parameters, $(\mathcal{A}_s)_{e\mu}$, $(\mathcal{A}_c)_{e\mu}$, $(\mathcal{B}_s)_{e\mu}$, and $(\mathcal{B}_c)_{e\mu}$ are sidereal time dependent, and $(\mathcal{C})_{e\mu}$ is a sidereal time independent parameter. The baseline of neutrinos is L, and $\omega_\oplus$ is the sidereal time angular frequency described shortly. These parameters are expressed in terms of SME coefficients and directional factors [22]. The same formula describes the $\bar{\nu}_\mu \to \bar{\nu}_e$ oscillation probability by switching the signs of the CPT-odd SME coefficients.

For this analysis, we convert the standard GPS time stamp for each event to local solar time (period 86400.0 sec) and sidereal time (period 86164.1 sec). We then define the local solar time angular frequency $\omega_\odot = \frac{2\pi}{86400.0}$ (rad/s) and the sidereal time angular frequency $\omega_\oplus = \frac{2\pi}{86164.1}$ (rad/s). The time origin can be arbitrary, but we follow the standard convention with a Sun-centered coordinate system [6]. We choose a time-zero of 58 min after an autumnal equinox of 2002 (September 23, 04:55GMT), so that this serves not only as the sidereal time-zero, but also as the solar time-zero since Fermilab is

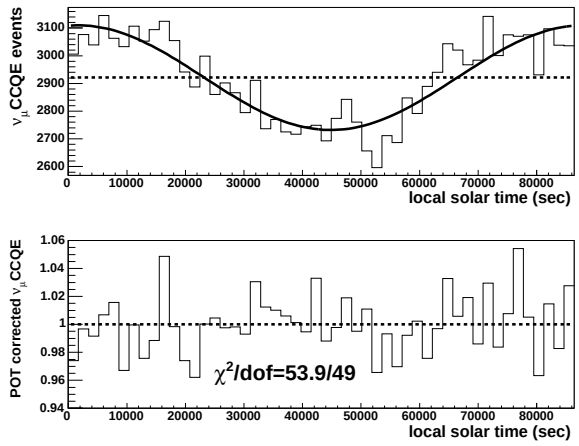

FIG. 1: The top plot shows the ν_μCCQE local solar time distribution. The bottom plot shows the same events after correcting for variations in POT. The χ^2 of this distribution with a flat hypothesis is 53.9/49 (29.3% compatibility).

	low energy		high energy		combined	
	solar	sidereal	solar	sidereal	solar	sidereal
Neutrino mode						
$< E_\nu >$	0.36 GeV		0.82 GeV		0.71 GeV	
#evt	544		420		964	
P(KS)	0.42	0.13	0.81	0.64	0.64	0.14
Anti-neutrino mode						
$< E_{\bar\nu} >$	0.34 GeV		0.78 GeV		0.60 GeV	
#evt	119		122		241	
P(KS)	0.62	0.15	0.79	0.39	0.69	0.08

TABLE I: A summary of K-S test results on the sidereal and local solar time distributions. The top table is for ν_e candidate data, and the bottom table is for $\bar\nu_e$ candidate data. The three rows show the average neutrino energy of each sample, number of events, and the K-S test compatibility with the null hypothesis. The test is performed in three energy regions, and for both solar local time and sidereal time distributions.

on the midnight point at this time. The local coordinate of the BNB are specified by three angles [22], colatitude $\chi = 48.2°$, polar angle $\theta = 89.8°$, and azimuthal angle $\phi = 180.0°$.

Any time dependent background variation, such as the time variation of detector and BNB systematics, are important. To evaluate these, we use our high statistics ν_μCCQE sample (Figure 1, top). This data sample is the same as our ν_μCCQE double differential cross section measurement sample [23] composed of 146,070 events (5.58×10^{20} POT). The ν_μCCQE local solar time distribution exhibits $\pm 6\%$ variation. The same variation in local solar time is observed in the POT. After correcting for variations in the POT, the resulting ν_μCCQE distribution in local solar time is consistent with a flat distribution (Figure 1, bottom). Due to the extensive running time of MiniBooNE (8 years), the variation in solar time is completely lost when the $\nu_\mu$events are plotted in sidereal time. The much lower statistics of the ν_e ($\bar\nu_e$) signal candidates further reduce the impact of any day-night variations to a negligible level in either solar or sidereal time, therefore no correction is applied in the analysis of ν_e ($\bar\nu_e$) candidate events that follows.

To check for a general deviation from a flat distribution (null sidereal variation hypothesis), we perform an unbinned Kolmogorov-Smirnov test (K-S test) [24] as a statistical null hypothesis test for both the ν_e and $\bar\nu_e$ samples. The K-S test is suitable in our case because it is sensitive to runs in distributions, which may be a characteristic feature of the sidereal time dependent hypothesis. Table I gives the result. The K-S test is applied to the low energy, high energy, and combined regions, for both neutrino, and anti-neutrino mode data. To investigate the time dependent systematics, we also apply the K-S test to the local solar time distribution. The test shows none of the twelve samples has less than 5% compatibility ($\sim 2\sigma$), which we chose as a benchmark prior to the analysis. Hence, all samples are compatible with the null sidereal variation hypothesis. Interestingly, the sidereal time distributions tend to show lower compatibility with a flat hypothesis, but not by a statistically significant amount. These results indicate that any sidereal variation extracted from our data, discussed below, is not expected to be statistically significant.

To fit the data with the sidereal time-dependent model, we use a generalized unbinned maximum likelihood method [25]. This method finds the best fit model parameters by fitting data with a log likelihood function ℓ. It is suitable for our analysis because this method has the highest statistical power for a low statistics sample. In this method, the log likelihood function ℓ is constructed by adding ℓ_i from each event. After dropping all constants, ℓ_i has the following expression,

$$\ell_i = -\frac{1}{N}(\mu_s + \mu_b) + ln[\mu_s \mathcal{F}_s^i + \mu_b \mathcal{F}_b^i] - \frac{1}{2N}\left(\frac{\mu_b - \overline{\mu_b}}{\sigma_b}\right)^2 . \quad (3)$$

Here, N is the number of observed candidate events, μ_s is the predicted number of signal events, μ_b is the predicted number of background events, $\mathcal{F}_s$ is the probability density function (PDF) for the signal and is a function of sidereal time and the fitting parameters (Eq. 2 with proper normalization), $\mathcal{F}_b$ is the PDF for the background, σ_b is the 1σ error on the predicted background, and $\overline{\mu_b}$ is the central value of the predicted total background events. The parameter space is scanned (grid search method) to find the largest ℓ, or the maximum log likelihood (MLL) point, and this MLL point provides the combination of the best fit (BF) parameters. The log likelihood function includes six parameters, five that are functions of SME coefficients, and one for the background. However the background term is constrained

within a $\pm 1\sigma$ range. Neither the neutrino nor the anti-neutrino mode data allow us to extract errors if we fit all five parameters at once, due to the high correlation of parameters. Therefore, we set $(\mathcal{B}_s)_{e\mu}$ and $(\mathcal{B}_c)_{e\mu}$ to zero and concentrate on three parameters ($(\mathcal{C})_{e\mu}$, $(\mathcal{A}_s)_{e\mu}$, and $(\mathcal{A}_c)_{e\mu}$) for the uncertainty estimates. Since the five parameter fit is quantitatively similar to the three parameter fit, we will focus the discussion on the results on the three parameter fits. This three parameter fit also corresponds to the case with only CPT-odd SME coefficients [22].

Figure 2 shows the neutrino mode low energy region fit results. The top three plots show the three projections of three dimensional parameter space. Because of the square of fitting parameters in the PDF, the BF point has a sign ambiguity and is always duplicated. The 1σ and 2σ contours are formed from a constant slice of the log likelihood function in the three dimensional parameter space. These slices enclose 68% (1σ) or 95% (2σ) of BF points for the three parameter fit of simulated, or "fake" data sets with the signal. Note that because fitting parameters are not linear in the PDF, twice the 1σ error does not yield the 2σ error.

A null sidereal variation hypothesis, or a flat solution, is equivalent to a three or five parameter fit solution where only the $(\mathcal{C})_{e\mu}$ parameter is nonzero. The fit to neutrino data favors a nonzero solution only for the $(\mathcal{C})_{e\mu}$ term. The bottom plot in Figure 2 shows data plotted against curves corresponding to the flat solution and the best fits for three and five parameter functions. Since all three curves are close to each other, the solution of neutrino mode is dominated by the sidereal time-independent component. To find the significance of time dependence over the flat distribution, fake data sets without the signal are formed where the ν_e candidate events are simulated without any time structure. The MLL difference between the three parameter fit and flat solution is used to form a $\Delta\chi^2$, and the expected $\Delta\chi^2$ distribution is determined by testing 500 random distributions from the fake data sets. This test shows that there is a 26.9% chance that a random distribution of ν_e candidate events would yield a $\Delta\chi^2$ value equal to, or greater than, the value observed for the data.

Figure 3 shows the analogous fit results for the anti-neutrino mode combined energy region. Due to lower statistics, the combined region is used rather than dividing the data into two subsets. Unlike the neutrino mode low-energy region, the $(\mathcal{C})_{e\mu}$ parameter no longer significantly deviates from zero. The fit to anti-neutrino data favors a non-zero solution for the $(\mathcal{A}_s)_{e\mu}$ and $(\mathcal{A}_c)_{e\mu}$ parameters at the nearly 2σ level. Performing the same $\Delta\chi^2$ test as is outlined above results in only 3.0% of the random distributions from the $\bar{\nu}_e$ candidate events having a $\Delta\chi^2$ value exceeding the value observed for the data. Note that this is consistent with the 8% compatibility with a flat hypothesis found with the K-S test (Tab. I).

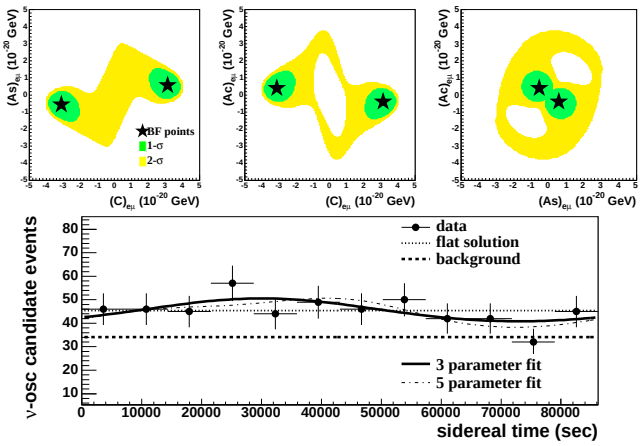

FIG. 2: (color online) Three parameter fit results for the neutrino mode low energy region. The top three plots show the projection of three dimensional parameter space. The dark (light) shaded area shows the 1σ (2σ) contour in each projection. The stars show the BF points. The bottom plot shows the curves corresponding to the flat solution (dotted), three parameter fit (solid), and five parameter fit (dash-dotted), together with binned data (marker). Here, the fitted background is shown as a dashed line, and the BF value is 1.00 (*i.e.*, equivalent to the central value of the predicted background).

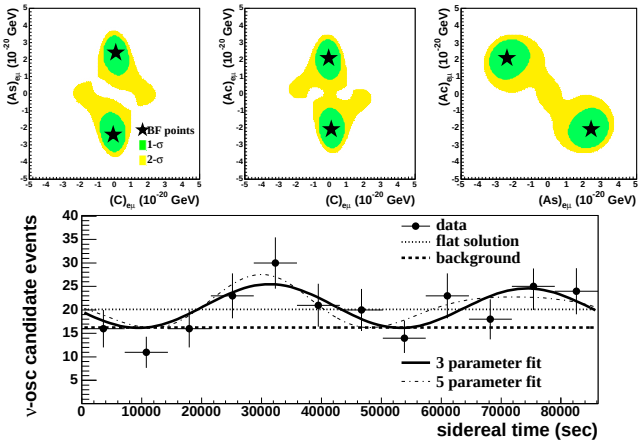

FIG. 3: Three parameter fit results for the anti-neutrino mode combined region. Notations are the same as Fig. 2. Here, the BF value for the fitted background is 0.97 (3% lower than the central value of the predicted background).

Table II shows fit parameters for the neutrino mode low energy region and anti-neutrino mode combined region. All errors are estimated from 1σ contours of parameter space projections. Errors are asymmetric, but we choose the larger excursions as the symmetric errors for simplicity. The 2σ contours provide the limits. In principle, these fit parameters are complex numbers. Here all pa-

	$\nu-$mode BF	2σ limit	$\bar{\nu}-$mode BF	2σ limit	SME coefficients combination (unit 10^{-20} GeV)
$\lvert(\mathcal{C})_{e\mu}\rvert$	$3.1 \pm 0.6 \pm 0.9$	< 4.2	$0.1 \pm 0.8 \pm 0.1$	< 2.6	$\pm[(a_L)^T_{e\mu} + 0.75(a_L)^Z_{e\mu}] - < E > [1.22(c_L)^{TT}_{e\mu} + 1.50(c_L)^{TZ}_{e\mu} + 0.34(c_L)^{ZZ}_{e\mu}]$
$\lvert(\mathcal{A}_s)_{e\mu}\rvert$	$0.6 \pm 0.9 \pm 0.3$	< 3.3	$2.4 \pm 1.3 \pm 0.5$	< 3.9	$\pm[0.66(a_L)^Y_{e\mu}] - < E > [1.33(c_L)^{TY}_{e\mu} + 0.99(c_L)^{YZ}_{e\mu}]$
$\lvert(\mathcal{A}_c)_{e\mu}\rvert$	$0.4 \pm 0.9 \pm 0.4$	< 4.0	$2.1 \pm 1.2 \pm 0.4$	< 3.7	$\pm[0.66(a_L)^X_{e\mu}] - < E > [1.33(c_L)^{TX}_{e\mu} + 0.99(c_L)^{XZ}_{e\mu}]$

TABLE II: The fit parameters for the neutrino mode low energy region and the anti-neutrino mode combined region. The BF points are the MLL points of the log likelihood function, and 1σ statistical and systematic errors are shown as well as 2σ limits. Detailed expressions of each sidereal fit parameter are shown in terms of SME parameters, and directional factors [22]. The upper (lower) sign of $(a_L)^\lambda_{e\mu}$ terms is applied for neutrino (anti-neutrino) results, due to the CPT-odd nature. The average neutrino energy "$< E >$" is 0.36 GeV for the neutrino mode low energy region and 0.60 GeV for the anti-neutrino mode combined region (Tab. I).

rameters are assumed to be real. A naive estimation from Tab. II indicates possible SME coefficients to satisfy the MiniBooNE data are of order 10^{-20} GeV (CPT-odd), and 10^{-20} to 10^{-19} (CPT-even). However, these SME coefficients are too small to produce a visible effect for LSND [6]. On the other hand, any SME coefficients extracted from LSND [6] predict too large of a signal for MiniBooNE. Therefore, a simple picture using Lorentz violation to explain both data sets leaves some tension, and a mechanism to cancel the Lorentz violating effect at high energy [3, 18, 19] is needed.

In summary, we performed a sidereal time variation analysis for MiniBooNE ν_e and $\bar{\nu}_e$ appearance candidate data. For the neutrino mode low energy region, K-S test statistics indicate the null hypothesis is compatible at the 13% level, and the relative improvement in the likelihood between the null hypothesis and the three parameter fit occurs 26.9% of the time in random distributions from a null hypothesis. Analysis of the combined energy region in anti-neutrino mode results in a K-S test that indicates a 8% compatibility with the null hypothesis, however the relative improvement in the likelihood between the null hypothesis and the three parameter fit only occurs 3.0% of the time in random distributions from a null hypothesis. The limit of fit parameters, 10^{-20} GeV, is consistent with Planck scale suppressed physics, and is currently the best limit for both $\nu_\mu \to \nu_e$ and $\bar{\nu}_\mu \to \bar{\nu}_e$ oscillations. This limit can be significantly improved by long baseline ν_e ($\bar{\nu}_e$) appearance experiments, such as T2K [26] and NOvA [27].

This work was conducted with support from Fermilab, the U.S. Department of Energy, and the National Science Foundation.

[1] V. A. Kostelecký and S. Samuel, Phys. Rev. D **39**, 683 (1989).

[2] S. Coleman and S. L. Glashow, Phys. Rev. D **59**, 116008 (1999).

[3] V. A. Kostelecký and M. Mewes, Phys. Rev. D **69**, 016005 (2004).

[4] A. A. Aguilar-Arevalo *et al.*, Phys. Rev. Lett. **98**, 231801 (2007); Phys. Rev. Lett. **102**, 101802 (2009).

[5] A. A. Aguilar-Arevalo *et al.*, Phys. Rev. Lett. **103**, 111801 (2009); Phys. Rev. Lett. **105**, 181801 (2010).

[6] L. B. Auerbach *et al.*, Phys. Rev. D **72**, 076004 (2005).

[7] P. Adamson *et al.*, Phys. Rev. Lett. **101**, 151601 (2008); Phys. Rev. Lett. **105**, 151601 (2010).

[8] R. Abbasi *et al.*, Phys. Rev. D **82**, 112003 (2010).

[9] V. A. Kostelecký and M. Mewes, Phys. Rev. D **70**, 031902 (R) (2004).

[10] A. A. Aguilar-Arevalo *et al.*, Phys. Rev. D **79**, 072002 (2009).

[11] A. A. Aguilar-Arevalo *et al.*, Nucl. Instrum. Meth. A **599**, 28 (2009).

[12] R. B. Patterson *et al.*, Nucl. Instrum. Meth. A **608**, 206 (2009).

[13] A. A. Aguilar-Arevalo *et al.*, Phys. Rev. Lett. **100**, 032301 (2008).

[14] `http://www-boone.fnal.gov/for_physicists/data_release`

[15] A .A. Aguilar-Arevalo *et al.*, Phys. Rev. D **64**, 112007 (2001).

[16] J. Kopp *et al*, arXiv:1103.4570 [hep-ph].

[17] O. W. Greenberg, Phys. Rev. Lett, **89**, 231602 (2002).

[18] T. Katori *et al.*, Phys. Rev. D **74**, 105009 (2006).

[19] J. S. Díaz and V. A. Kostelecký, Phys. Lett. B **700**, 700 25 (2011); arXiv:1108.1799 [hep-ph].

[20] D. Colladay and V. A. Kostelecký, Phys. Rev. D **55**, 6760 (1997); Phys. Rev. D **58**, 116002 (1998); V. A. Kostelecký, Phys. Rev. D **69**, 105009 (2004).

[21] For recent reviews see, for example, *CPT and Lorentz Symmetry V*, edited by V. A. Kostelecký, (World Scientific, Singapore, 2011); V. A. Kostelecký and N. Russell, Rev. Mod. Phys. **83**, 11 (2011).

[22] V. A. Kostelecký and M. Mewes, Phys. Rev. D **70**, 076002 (2004).

[23] A. A. Aguilar-Arevalo *et al.*, Phys. Rev. D **81**, 092005 (2010).

[24] W. H. Press *et al.*, *Numerical Recipes in C++: The Art of Scientific Computing*, (Cambridge University Press, New York, 2002).

[25] L. Lyons, *Statistics for Nuclear and Particle Physicists*, (Cambridge University Press, New York, 1989).

[26] K. Abe *et al.*, Phys. Rev. Lett. **107**, 041801 (2011).

[27] D. S. Ayres *et al.*, arXiv:hep-ex/0503053.